This is a preproof accepted article for *Mineralogical Magazine*

This version may be subject to change during the production process

DOI: 10.1180/mgm.2025.10165

Sarvodaite $Al_2(SO_4)_3 \cdot 5H_2O$, a new mineral from the Fan-Yagnob coal deposit, Tajikistan

Saimudasir Makhmadsharif[1,2], Leonid A. Pautov[3], Oleg I. Siidra[4,5*], Mirak A. Mirakov[1], Vladimir Yu. Karpenko[3], Manuchekhr A. Shodibekov[1]

[1]Institute of Geology, Earthquake Engineering and Seismology, Academy of Sciences of the Republic of Tajikistan, Aini 267, 734063, Dushanbe, Tajikistan.

[2]Russian State Geological Prospecting University, MGRI, Miklouho-Maclay ul. 23, 117997, Moscow, Russia.

[3]Fersman Mineralogical Museum, Russian Academy of Sciences, Leninskiy pr. 18-2, 119071 Moscow, Russia.

[4]Department of Crystallography, St. Petersburg State University, University Emb., 7/9, St. Petersburg, 119034, Russia.

[5]Kola Science Center, Russian Academy of Sciences, Apatity, Murmansk Region, 184200 Russia, 683006, Russia.

* E-mail: o.siidra@spbu.ru

ABSTRACT

A new hydrous aluminium sulfate mineral sarvodaite, $Al_2(SO_4)_3 \cdot 5H_2O$, was discovered at the tract of Kukhi-Malik, Fan-Yagnob coal deposit, ca. 75 km N of Dushanbe, Tajikistan. Sarvodaite is a fumarolic mineral formed directly from gas from a natural underground coal fire. Associated minerals are anhydrite, realgar, native selenium and several unknown phases. The mineral typically occurs as white spherolites of thin colorless prismatic crystals up to 500 μm in maximum dimension. Sarvodaite is optically biaxial, α = 1.529(2), β = 1.537(2), γ(calc.) = 1.545(3) (590 nm), and the measured 2V is 90(3)°. The measured density is 2.33(2) g/cm^3. The mineral is non-soluble in water and ethanol and dissolves slowly at room temperature in HCl. The composition of sarvodaite was studied using EDS. Raman and IR spectroscopy confirmed the presence of H_2O. The empirical formula calculated on the basis of 17 O atoms per formula unit is $(Al_{1.88}Fe_{0.06}Ti_{0.04})_{\Sigma 1.98}S_{3.01}O_{12} \cdot 5H_2O$.

Sarvodaite is monoclinic, $P2_1/n$, a = 5.4862(4), b = 10.8029(8), c = 20.8413(15) Å, β = 96.416(7)°, V = 1227.46(16) Å^3, Z = 4. The structure of sarvodaite contains three symmetrically independent Al sites and three S site. Al-centered octahedra and sulfate groups form strongly corrugated layers interconnected via hydrogen bonding. Sarvodaite has a synthetic analogue. Infrared and Raman spectra are reported.

Sarvodaite is the third hydrous Al sulfate mineral species without additional cations and anions to be described to date, following alunogen, $Al_2(SO_4)_3 \cdot 17H_2O$ and metaalunogen, $Al_2(SO_4)_3 \cdot 12H_2O$.

Keywords: sarvodaite; sulfates; hydrates; natural coal fires, sublimates, Fan-Yagnob coal deposit.

Introduction

Sarvodaite, $Al_2(SO_4)_3 \cdot 5H_2O$, a new mineral, was discovered in the sublimates of a natural underground coal fire in the upper reaches of the Kukhi-Malik tract in the Ravat area of the Fan-Yagnob coal deposit, Tajikistan. The new mineral is named after the ancient Sarvoda fortress, the remains of which are situated in the vicinity to the place where sarvodaite was found, the village of Zeravshan-Sarvoda. In the Middle Ages, this fortress served as an outpost on the route to the "burning mines", which were referred to by various names at different eras (Kan-Tag, Ravat, Kukhi-Malik). The region was the source of the extraction of ammonia, native sulfur, potassium nitrate, alum, and iron sulfate from ancient times until the mid-40s of the 20th century. These minerals were employed in the production of gunpowder, the pollination of vineyards, the processing of leather, and the production of medicine. In the Sarvoda fortress, the sublimations were processed by local residents (Ermakov, 1935; Novikov and Suprychev, 1986). The mineral and its name were approved by the Commission on New Minerals, Nomenclature and Classification of the International Mineralogical Association (CNMNC IMA) (IMA 2023-073). The holotype of the sarvodaite under investigation is housed in the collections of the Fersman Mineralogical Museum (Moscow), with the reference number 6041/1.

A comprehensive analysis of crystallographic characteristics of all known hydrated aluminum sulfates, including those containing OH groups, was recently performed in Mauro et al. (2023). Alunogen, $Al_2(SO_4)_3 \cdot 17H_2O$ and metaalunogen, $Al_2(SO_4)_3 \cdot 12H_2O$ are the only two known to date natural hydrous aluminum sulfates that do not contain additional cations and anions. Monoclinic $Al_2(SO_4)_3 \cdot 5H_2O$ is a synthetic analogue of sarvodaite that was

https://doi.org/10.1180/mgm.2025.10165 Published online by Cambridge University Press

synthesized by evaporating a mixture of $Al_2(SO_4)_3 \cdot 7H_2O$ with sulfuric acid and subsequently subjecting the products to hydrothermal treatment in an autoclave at a temperature of 180 °C (Fischer et al., 1996). Witzke et al. (2015) reported the discovery of a phase with the composition $Al_2(SO_4)_3 \cdot 5H_2O$ in a dense, white, pumice-like aggregate of godovikovite–millosevichite from the dumps of the Burning Anna I Coal Mine Dump in Alsdorf, Germany.

Occurrence

Figure 1. Location of Kukhi-Malik (a). "Big Grotto" gas vent where sarvodaite was found (b). The panorama depicts the right side of the river Fan-Darya, with a view of Kukhi-Malik (marked with a red circle). The village of Ravat is visible below, and the snow-covered Fann Mountains are in the background (c).

Sarvodaite was found in sublimates during the fieldwork in 2023. The mineral was discovered in the upper reaches of the Kukhi-Malik tract (Fig.1a-c) on the right bank of the Fan Darya River (39°12′25″ N, 68°33′59″ E) in the contours of the Fan-Yagnob coal deposit, where hot coal gases were released from an underground fire in the "Big Grotto" gas vent (Fig. 1b). Sarvodaite was discovered on the walls of a crack in burnt sandstones. The temperature of the gas flow was in the range from 100 to 220 °C. All samples were immediately sealed in glass tubes upon their collection to prevent any potential exposure to the external environment. Within the Fan-Yagnob coal deposit, which spans roughly 10 hectares on both the left and right banks of the Fan Darya River, natural underground coal

https://doi.org/10.1180/mgm.2025.10165 Published online by Cambridge University Press

fires are common. Along with the over 200 gas vents that are currently active, there are numerous outlets for coal combustion products, as well as new fire areas that are established annually. The natural underground fire at Ravat is believed to have been ongoing for over 2000 years (Novikov and Suprychev, 1986). Presently, industrial coal mining is conducted on the left river bank, while manual mining is conducted on the right side, with a length of 400 meters. Predominantly, low-temperature sublimations associated with near-surface coal fire are observed on the left bank of the river. The primary products are sulfur, ammonia, alum, sulfuric acid that impregnates the soil, and a variety of organic compounds with relatively low crystallization temperatures, such as ravatite (Nasdala and Pekov, 1993), which produce a distinctive pungent odor in sublimates. Areas on the right bank of the Fan-Darya River in the upper reaches of the Kukhi-Malik tract are characterized by the higher sublimate formation temperatures. Paralavas, sedimentary rock melting products, are abundant in the Ravat area of the deposit (Sharygin et al., 2009). Numerous publications have reported the mineralogy of sublimates from natural underground coal fires at the Fan-Yagnob deposit (Ermakov, 1935; Novikov et al., 1979; Belakovski, 1990; Mirakov et al., 2019; Pautov et al., 2020; Karpenko et al., 2023; Mirakov et al., 2023).

Associated minerals and physical properties

Associated minerals are anhydrite, realgar, native selenium and several unknown phases. Sarvodaite typically occurs as white spherolites (Fig. 2a,b) of thin colorless prismatic crystals (Fig. 2c) up to 500 μm in maximum dimension. The streak is white. The luster is vitreous. Sarvodaite is brittle. Cleavage is perfect on {100}. The fracture is splintery. Hardness is 1-1½. The tiny size of the crystals makes it impossible to measure the microhardness. Tiny sarvodaite crystals display cracks that are parallel to their elongation; these cracks may be misinterpreted as the intergrowth planes of multiple crystals or a cleavage.

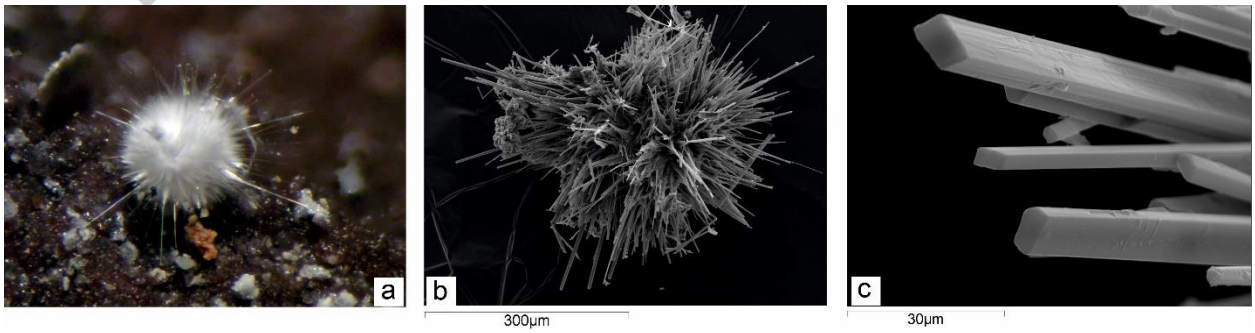

https://doi.org/10.1180/mgm.2025.10165 Published online by Cambridge University Press

Figure 2. White sarvodaite spherolite (field of view 1.8 mm) (a). SEM images of sarvodaite spherolite (b) and prismatic crystals (c).

Sarvodaite is optically biaxial (-/+ unclear) (Fig. 3), α = 1.529(2), β = 1.537(2), γ(calc.) = 1.545(3) (590 nm), and the measured 2V is 90(3)°. The mineral shows straight extinction on sections with positive elongation, while the extinction is oblique on sections with negative elongation ($C:N_m$ = 10°). Dispersion is weak, r > v. The mineral is non-pleochroic under the microscope. The measured density is 2.33(2) g/cm^3. The density calculated based on the empirical formula of the holotype is 2.349 g/cm^{-3}. The Gladstone-Dale compatibility index, $1 - (K_p/K_c)$ = -0.010, is superior.

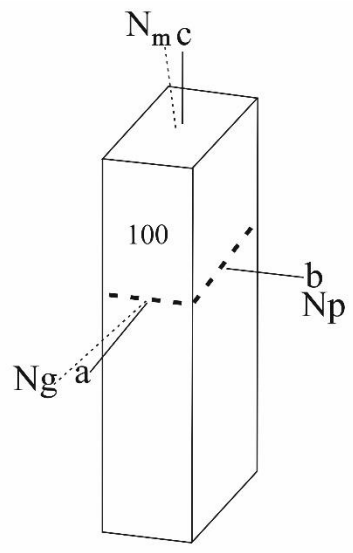

Figure 3. The optical orientation of the sarvodaite crystal. The plane of the optical axes is depicted by the dotted line.

Infrared and Raman spectroscopy

The IR spectrum of sarvodaite (Fig. 4) was obtained from a KBr microtablet using an FSM 2201 Fourier transform IR spectrometer (Infraspec, Russia). Four regions of bands are observed in the IR spectra of sarvodaite:

(1) An intensive and broad absorption band with many shoulders in the 2900-3500 cm^{-1} region corresponding to stretching vibrations of water molecules;

(2) An intense band at 1600-1700 cm^{-1} corresponding to deformation vibrations in water molecules;

(3) Several intensive bands in the 900-1300 cm^{-1} range associated with stretching vibrations of the sulfate group;

https://doi.org/10.1180/mgm.2025.10165 Published online by Cambridge University Press

(4) A number of bands in the 400-700 cm^{-1} region associated with deformation vibrations of the sulfate group, respectively. Bands at 758 and 852 cm^{-1} may be attributed to Al–O vibrations (Kloprogge et al., 2001; Košek et al., 2018).

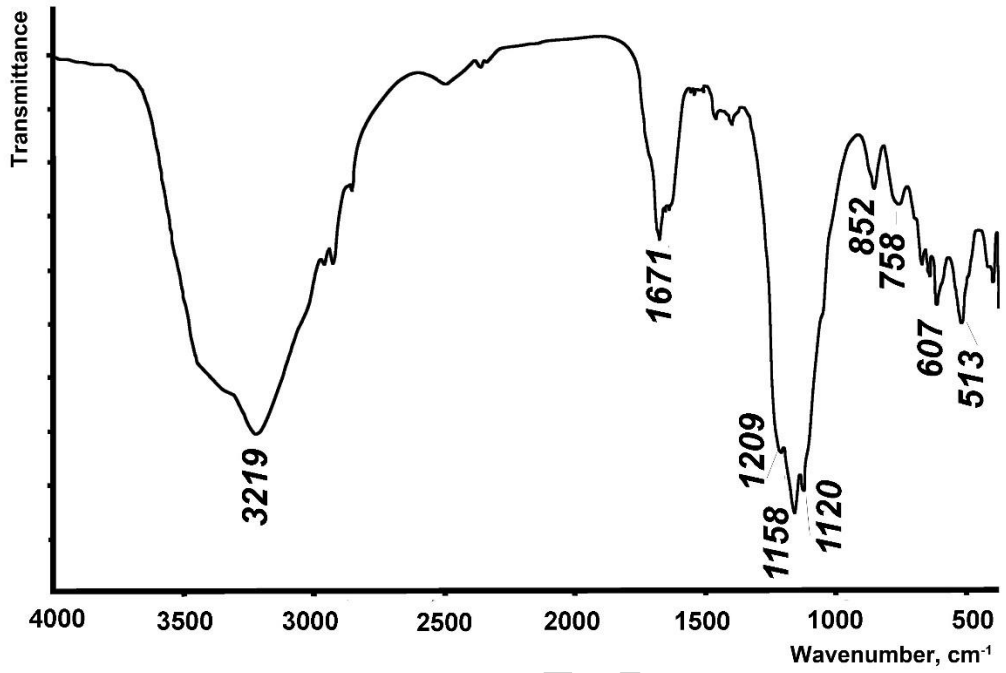

Figure 4. IR spectra of sarvodaite.

The Raman spectra (Fig. 5) were obtained on a sarvodaite single crystal that was extracted from the sample for the single-crystal X-ray study. The following are the instruments and analysis parameters: DXR2xi Thermo Scientific Raman Imaging Microscope in the range of 6000 cm^{-1} to 50 cm^{-1} using 2 cm^{-1} resolution, 25 μm pinhole aperture, grating of 400 lines/mm, and scan time of 0.5 s with 40 scans. In order to protect the sample from destruction, a laser with a wavelength of 532 nm was used at 70% power at the sample (7 mW). The sample surface did not sustain any damage. Identical Raman spectra were obtained from four different areas of the crystal surface. The Si standard was used for the calibration. The tentative assignment of Raman bands was performed using available data for alunogen $Al_2(SO_4)_3 \cdot 17H_2O$ and other Al-sulfates (Frost et al., 2015; Košek et al., 2018, 2022). Bands in the region 3200–3450 cm^{-1} can be assigned as O-H stretching vibrations of water molecules. In the obtained Raman spectra, the ν_1 and ν_3 sulfate modes are assigned to narrow bands in the range 1200-1000 cm^{-1}, the ν_4 sulfate mode is assigned to 646 cm^{-1}, and the ν_2 modes are assigned to a series of non-intensive bands in the range 400-500 cm^{-1}. Lattice vibrations are responsible for weaker bands in the range of less than 400 cm^{-1}.

https://doi.org/10.1180/mgm.2025.10165 Published online by Cambridge University Press

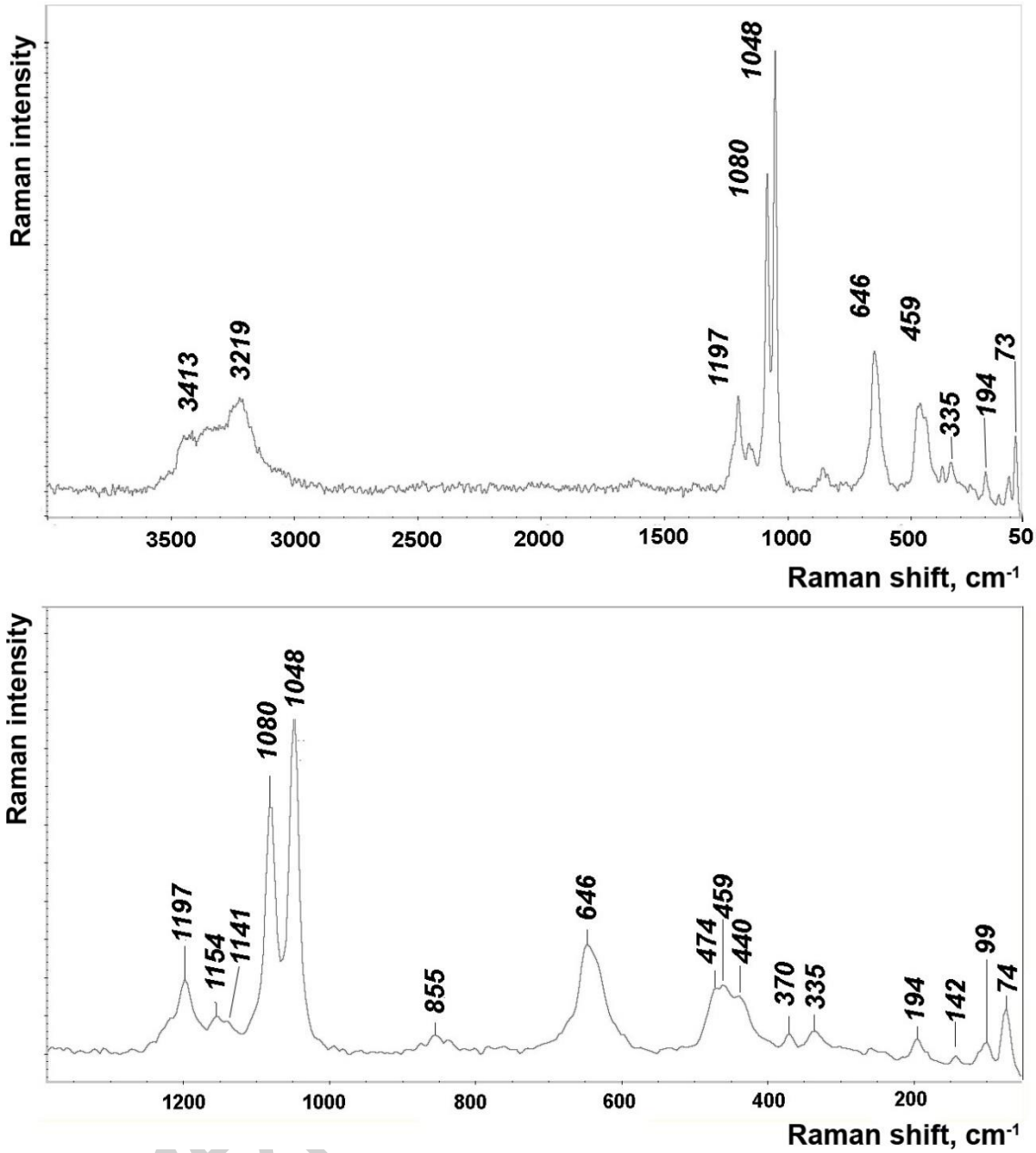

Figure 5. Raman spectra of sarvodaite.

Chemistry

Crystals of sarvodaite were mounted in epoxy resin and polished. The composition of sarvodaite (Table 1) was studied using a Superprobe JCXA-733 scanning electronic microscope equipped with an Oxford Instruments INCA Energy Dispersive Spectrometer (EDS) and JCXA-733 (JEOL) analyzer with a Si-(Li) detector with ATW2 ultrathin window and INCA Energy 350 analysis system (20 kV accelerating voltage, 0.5 nA electron beam current measured with a Faraday cup and a beam of 10 μm were used for the analysis). $BaSO_4$ (S*K*α), TiO_2 (Ti*K*α), Fe_2O_3 (Fe*K*α) and Al_2O_3 (Al*K*α) were used as standards.

https://doi.org/10.1180/mgm.2025.10165 Published online by Cambridge University Press

The empirical formula calculated on the basis of 17 O atoms per formula unit is $(Al_{1.88}Fe_{0.06}Ti_{0.04})_{\Sigma 1.98}S_{3.01}O_{12}\cdot 5H_2O$. The simplified formula is $(Al,Fe)_2(SO_4)_3\cdot 5H_2O$. The ideal formula is $Al_2(SO_4)_3\cdot 5H_2O$, which requires Al_2O_3 23.59; SO_3 55.57; H_2O 20.84; Total 100 wt.%.

The mineral is non-soluble in water and ethanol. Sarvodaite dissolves slowly at room temperature in HCl 1:1.

Crystallography

Powder X-ray diffraction data were collected using Cr*K*α radiation with a V-filter in a RKU-86 camera; Ge was used as an internal standard. The results are given in Table 2. Unit-cell parameters refined from the powder data are as follows: monoclinic, a = 5.48(2), b = 10.803(5), c = 20.84(1) Å, β = 96.42(3), V = 1227(1) Å^3. MID-2 software was used to refine the unit-cell parameters.

A crystal of sarvodaite (Table 3) was mounted on a thin glass fibre for X-ray diffraction analysis using a Rigaku Synergy S diffractometer, with a micro-focus X-ray tube equipped with a CCD detector (Mo*K*α radiation) operated at 50 kV and 1 mA at the Department of Crystallography, St. Petersburg State University. More than a hemisphere of three-dimensional XRD data was collected with 200 s count time for each frame. Fractional atom coordinates and atomic displacement parameters are listed in Tables 4,5. Selected interatomic distances are given in Table 6. Hydrogen bonds are provided in Table 7 and bond-valence calculations in Table 8. The crystallographic information file has been deposited with the Principal Editor of Mineralogical Magazine and is available as Supplementary material (see below).

The unit-cell parameters of sarvodaite (Table 3) are nearly identical to those obtained for the synthetic analogue in Fischer et al. (1996) ($P2_1/n$, a = 5.4843(2), b = 10.7958(3), c = 20.8427(4) Å, β = 96.44(8)°, V = 1226.26 Å)^3. As an initial structure model, the atomic coordinates of Al, S and O atoms were taken from Fischer et al. (1996). O–H distance restraints of 1.00 ± 0.005 Å were applied. The isotropic displacement parameters for hydrogen atoms were held constant at 0.05 Å^2. The structure of sarvodaite contains three symmetrically independent Al sites and three S site (Fig. 6). S^{6+} cations are tetrahedrally coordinated by four O atoms each. Al atoms have octahedral coordination environments. Al1 atom is coordinated by three H_2O molecules and three O atoms belonging to sulfate groups. Al2 and Al3 atoms have similar coordination environments thus forming regular $AlO_4(H_2O)_2$

https://doi.org/10.1180/mgm.2025.10165 Published online by Cambridge University Press

octahedra. The minor amounts of Fe and Ti detected by the microprobe (see above) could not be refined. Al-centered octahedra and sulfate groups form strongly corrugated layers stacked along [001] and shown in Figure 7. The layers are interconnected via hydrogen bonding.

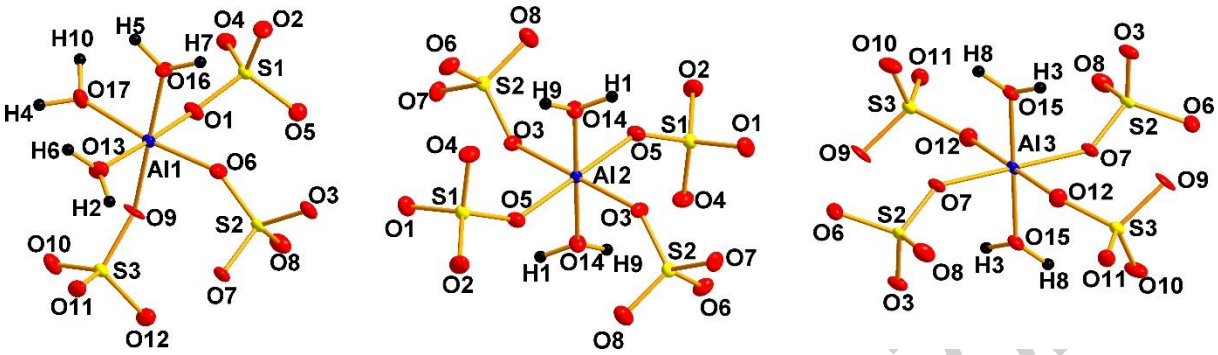

Figure 6. Coordination environments of Al and S atoms in the structure of sarvodaite. Ellipsoids are shown at 50% probability level.

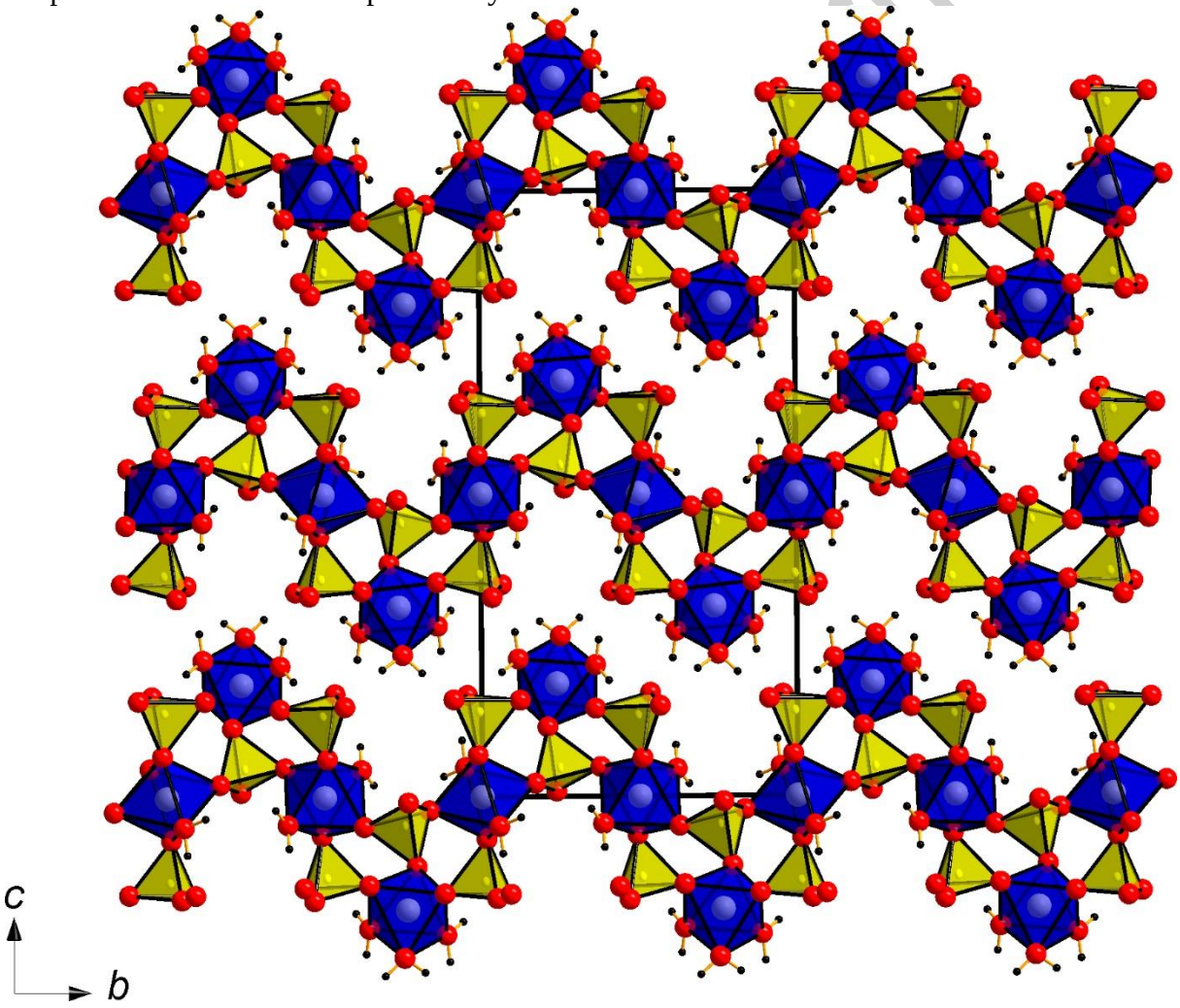

Figure 7. General projection of the crystal structure of sarvodaite (AlO_6 = blue, SO_4 = yellow, O atoms = red balls; H atoms = grey balls) along the *a* axis.

https://doi.org/10.1180/mgm.2025.10165 Published online by Cambridge University Press

Concluding remarks

Sarvodaite, a novel aluminum sulfate pentahydrate mineral species, was discovered in the sublimates of an underground coal fire. The mineral is believed to undergo direct crystallization as a result of the interaction between hot aerosol (sulfuric acid with water vapor) and the host rocks, which allows gases from the fire to escape to the surface. This is in contrast to the pseudomorphic formation of the $Al_2(SO_4)_3 \cdot 5H_2O$ phase in the dumps of the Anna1 coal mine after godovikovite (Witzke et al., 2015). The absence of any indications of sarvodaite crystallization after any primary minerals and the automorphic form of sarvodaite segregations (spherolites of well-formed needle-shaped crystals) support this assumption. Crystallization of sarvodaite at Kukhi-Malik occurs in hot coal gas discharge zones where the temperature drops below 200 °C but exceeds 100 °C. The temperature range in which sarvodaite is formed is consistent with the readily available data on the synthesis of $Al_2(SO_4)_3 \cdot 5H_2O$ at 180 °C (Fischer et al., 1996).

Acknowledgements

We acknowledge Elena Zhitova for the editorial handling and four anonymous reviewers for their comments. Authors gratefully acknowledge A.R. Fayziyev, Yu.V. Gritsenko, P. Aminzoda, M.L. Gadoev and Sh.Yo. Yorov for the help and joint field works at the Fan-Yagnob deposit. This work was financially supported by the Russian Science Foundation through the grant 25-17-00157 (for OIS). Technical support by the SPbSU X-ray Diffraction Resource Center (project # 118201839) and Research center for ecology and environment of Central Asia (Dushanbe) is gratefully acknowledged.

References

Belakovski D. (1990) Die Mineralien der brennenden Kohleflöze von Ravat in Tadshikistan. *Lapis*, **15**, 21-26.

Ermakov N.P. (1935) Pasrud-Yagnobskoye coal deposit and mines of the Kan-Tag mountain. In: On geology of coal deposits of Tajikistan. Materials of Tajik-Pamir Expedition 1933, **12**, 47-66 (in Russian).

Fischer T., Eisenmann B., Kniep R. (1996) Crystal structure of dialuminium tris (sulfate) pentahydrate, $Al_2(SO_4)_3 \cdot 5H_2O$. *Zeitschrift für Kristallographie-Crystalline Materials*, **211**, 471-472.

https://doi.org/10.1180/mgm.2025.10165 Published online by Cambridge University Press

Frost R.F., Scholz R., Lima R.M.F. and López A. (2015) SEM, EDS and vibrational spectroscopic study of the sulphate mineral rostite $AlSO_4(OH,F)\cdot 5(H_2O)$, *Spectrochimica Acta*, *A***151**, 616-620.

Gagné O.C. and Hawthorne F.C. (2015). Comprehensive derivation of bond-valence parameters for ion pairs involving oxygen. *Acta Crystallogr*. ***B*71**, 562-578.

Karpenko V.Yu., Pautov L.A., Siidra O.I., Mirakov M.A., Zaitsev A.N., Plechov P.Yu. and Makhmadsharif S. (2023) Ermakovite $(NH_4)(As_2O_3)_2Br$, a new exhalative arsenite bromide mineral from the Fan-Yagnob coal deposit, Tajikistan. *Mineralogical Magazine*, **87**, 69-78.

Kloprogge J.T., Ruan H. and Frost R.L. (2001) Near-infrared spectroscopic study of basic aluminum sulfate and nitrate. *Journal of Materials Research*, **36**, 603-607.

Košek F., Culka A., Rousaki A., Vandenabeele P. and Jehlička J. (2022) Raman spectroscopy of anhydrous and hydrated aluminum sulfates: Experience from burning coal heaps. *Journal of Raman Spectroscopy*, **53,** 1959-1973.

Košek F., Culka A., Žáček V., Laufek F., Škoda R. and Jehlička J. (2018). Native alunogen: A Raman spectroscopic study of a well-described specimen. *Journal of Molecular Structure*, **1157**, 191-200.

Mauro D., Biagioni C., Sejkora J., Dolníček Z., and Škoda R. (2023). Batoniite, $[Al_8(OH)_{14}(H_2O)_{18}](SO_4)_5\cdot 5H_2O$, a new mineral with the $[Al_8(OH)_{14}(H_2O)_{18}]^{10+}$ polyoxocation from the Cetine di Cotorniano Mine, Tuscany, Italy. *European Journal of Mineralogy*, **35**, 703-714.

Mirakov M.A., Pautov L.A., Karpenko V.Yu., Faiziev A.R. and Mahmadsharif S. (2019) Pauflerite β-$VO(SO_4)$ from sublimations of the natural underground fire at Kukhi-Malik (Ravat) tract, Fan-Yagnob coal deposit, Tajikistan. *New data on minerals*, **53**, 114-120 (in Russian).

Mirakov M.A., Pautov L.A., Siidra O.I., Makhmadsharif S., Karpenko V.Yu. and Plechov P.Yu. (2023) Hasanovite $KNa(MoO_2)(SO_4)_2$, a new mineral from natural underground coal fires at the Fan-Yagnob coal deposit, Tajikistan. *Proceedings of the Russian Mineralogical Society*, **152**, 18-36. In Russian with Eng. abstract.

Nasdala L. and Pekov I.V. (1993) Ravatite, $C_{14}H_{10}$, a new organic mineral species from Ravat, Tadzhikistan. *European Journal of Mineralogy*, **5**, 699-705.

https://doi.org/10.1180/mgm.2025.10165 Published online by Cambridge University Press

Novikov V.P., Suprychev V.V. and Babayev M.A. (1979) Salammoniac from sublimates of the underground coal fire at the Ravat coal deposit (Central Tadzhikistan). *Doklady Akademii nauk Tadzhikskoyi SSR*, **12**, 687 (in Russian).

Novikov V.P. and Suprychev V.V. (1986) Conditions of the modern mineral genesis at the underground firing coals at Fan-Yagnobskoye deposit. *Mineralogia Tadzhikistana*, **7**, 91-104 (in Russian).

Pautov L.A., Mirakov M.A., Siidra O.I., Faiziev A.R., Nazarchuk E.V., Karpenko V.Y. and Makhmadsharif S. (2020) Falgarite, $K_4(VO)_3(SO_4)_5$, a new mineral from sublimates of a natural underground coal fire at the tract of Kukhi-Malik, Fan-Yagnob coal deposit, Tajikistan. *Mineralogical Magazine*, **84**, 455-462.

Sharygin V.V., Sokol E.V. and Belakovski D.I. (2009) Fayalite–sekaninaite paralava from the Ravat coal fire (central Tajikistan). *Russian Geology and Geophysics*, **50**, 703–721.

Witzke T., de Wit F., Kolitsch U., Blass G. Mineralogy of the burning Anna I coal mine dump, Alsdorf, Germany. In Coal and Peat Fires - A Global Perspective. Edition: Volume 3. Case Studies - Coal Fires, Chapter 7. Editors: Stracher G.B., Prakash A., Sokol E.V. Elsevier, 2015, P. 203-240.

Table 1. Chemical data (in wt %) for sarvodaite.

Constituent	Mean	Range	Stand. Dev. (σ)	Reference Material
Al_2O_3	22.27	21.54 – 22.90	0.13	Al_2O_3
Fe_2O_3	1.08	0.77 – 1.50	0.09	Fe_2O_3
TiO_2	0.67	0.28 – 1.01	0.07	TiO_2
SO_3	55.86	53.73 – 57.35	0.20	$BaSO_4$
H_2O calc.*	20.93			
Total	100.81			

* based on structural data.

https://doi.org/10.1180/mgm.2025.10165 Published online by Cambridge University Press

Table 2. X-ray powder diffraction data (*d* in Å) for sarvodaite. Seven strongest lines are marked in bold.

I_{meas}	d_{meas}	I_{calc}	d_{calc}	*h*	*k*	*l*
45	**10.36**	**28**	**10.36**	**0**	**0**	**2**
100	**7.48**	**100**	**7.48**	**0**	**1**	**2**
35	5.40	34	5.40	0	2	0
3	4.85	2	4.85	-1	1	1
1	4.78	2	4.79	0	2	2
43	**4.64**	**52**	**4.64**	**1**	**1**	**1**
39	**4.56**	**49**	**4.53**	**-1**	**0**	**3**
5	3.99	20	4.06	1	0	3
58	**3.83**	**67**	**3.83**	**-1**	**2**	**1**
55	**3.74**	**50**	**3.74**	**0**	**2**	**4**
		25	**3.72**	**1**	**2**	**1**
50	**3.47**	**60**	**3.47**	**-1**	**2**	**3**
		22	**3.45**	**0**	**0**	**6**
24	3.40	29	3.40	0	3	2
6	3.32	8	3.32	-1	1	5
6	3.29	7	3.29	0	1	6
9	3.25	10	3.25	1	2	3
35	3.15	57	3.13	1	0	5
25	2.948	32	2.95	1	3	1
7	2.908	7	2.91	0	2	6
4	2.821	5	2.82	-1	3	3
14	2.730	12	2.73	-1	0	7
24	2.710	19	2.71	1	2	5
3	2.677	2	2.67	-1	3	4
8	2.646	5	2.64	2	1	0
5	2.614	5	2.61	0	4	2
3	2.568	2	2.56	-2	1	3
3	2.515	3	2.52	0	4	3
5	2.438	3	2.44	-1	2	7
5	2.421	4	2.42	-1	4	1
9	2.388	3	2.39	-1	1	8
3	2.346	3	2.35	-2	1	5
3	2.336	3	2.34	-1	3	6
6	2.310	8	2.31	2	0	4
6	2.267	9	2.27	-2	0	6
2	2.230	3	2.23	-1	2	8
2	2.183	2	2.18	-2	3	1

https://doi.org/10.1180/mgm.2025.10165 Published online by Cambridge University Press

4	2.173	5	2.17	2	3	0
1	2.151	2	2.15	0	5	1
2	2.126	3	2.12	0	5	2
6	2.102	8	2.10	0	3	8
9	2.072	7	2.07	0	0	10
3	2.032	3	2.03	2	0	6
5	1.992	5	1.99	1	5	1
2	1.960	2	1.96	1	5	2
7	1.944	9	1.94	2	3	4
2	1.909	2	1.91	1	5	3
2	1.830	3	1.83	1	4	7
1	1.802	2	1.80	0	3	10
6	1.756	11	1.75	2	4	4
4	1.747	5	1.75	-1	2	11
4	1.738	7	1.74	-2	4	6
3	1.715	2	1.72	1	0	11
4	1.682	1	1.68	2	5	1
5	1.675	7	1.67	-1	6	3
6	1.641	8	1.64	1	2	11
2	1.625	1	1.62	2	4	6
3	1.619	2	1.62	-2	1	11
2	1.603	1	1.60	-2	4	8
3	1.584	6	1.58	3	1	5
6	1.569	10	1.57	2	0	10

https://doi.org/10.1180/mgm.2025.10165 Published online by Cambridge University Press

Table 3. Crystallographic data and refinement parameters for sarvodaite.

Crystal data	
Formula	$Al_2S_3O_{17}H_{10}$
Crystal system	Monoclinic
Space group	$P2_1/n$ (no. 14)
Unit cell dimensions *a*, *b*, *c* (Å);	5.4862(4), 10.8029(8), 20.8413(15)
β (º)	96.416(7)
Unit-cell volume (Å^3)	1227.46(16)
Z	4
Absorption coefficient (mm^{-1})	0.851
Crystal size (mm)	0.01×0.01×0.07
Data collection	
Temperature (K)	150
Radiation, wavelength (Å)	MoKα, 0.71073
θ range (°)	3.502-27.999
h, *k*, *l* ranges	−7→7, −14→14, −27→27
Total reflections collected	11826
Unique reflections (R_{int})	2946 (0.07)
Unique reflections $F > 4\sigma(F)$	2053
F(000)	880
Structure refinement	
Refinement method	Full-matrix least-squares on F^2
Weighting coefficients *a*, *b*	0.0660, 2.5563
Data/restraints/parameters	2946 /10/232
R_1 [$F > 4\sigma(F)$], wR_2 [$F > 4\sigma(F)$]	0.0615, 0.1378
R_1 all, wR_2 all	0.0947, 0.1498
Gof on F^2	1.053
Largest diff. peak and hole (*e* Å^{-3})	0.824, −0.643

https://doi.org/10.1180/mgm.2025.10165 Published online by Cambridge University Press

Table 4. Coordinates, equivalent isotropic (U_{eq}) and isotropic (U_{iso}) displacement parameters (Å^2) of atoms in sarvodaite.

Atom	*Wyck.*	*x*	*y*	*z*	U_{eq}/U_{iso}*
Al1	4*e*	-0.0880(2)	-0.23870(13)	0.81354(6)	0.0109(3)
Al2	2*d*	-½	0	0	0.0090(4)
Al3	2*b*	-½	-½	0	0.0095(4)
S1	4*e*	0.20804(19)	0.00761(10)	0.85975(5)	0.0109(3)
S2	4*e*	-0.2703(2)	-0.24667(10)	0.95270(5)	0.0105(3)
S3	4*e*	0.1588(2)	-0.49418(11)	0.86657(5)	0.0117(3)
O1	4*e*	0.1578(6)	-0.1214(3)	0.84042(17)	0.0183(7)
O2	4*e*	0.0030(6)	0.0886(3)	0.83920(16)	0.0184(8)
O3	4*e*	-0.4555(6)	-0.1678(3)	0.97788(16)	0.0152(7)
O4	4*e*	0.4325(6)	0.0451(3)	0.83216(16)	0.0182(7)
O5	4*e*	0.2537(6)	0.0131(3)	0.93067(15)	0.0160(7)
O6	4*e*	-0.2550(6)	-0.2088(3)	0.88521(16)	0.0174(7)
O7	4*e*	-0.3590(6)	-0.3754(3)	0.95105(15)	0.0159(7)
O8	4*e*	-0.0358(6)	-0.2351(3)	0.99099(17)	0.0205(8)
O9	4*e*	0.1143(6)	-0.3605(3)	0.85452(17)	0.0186(8)
O10	4*e*	0.3534(6)	-0.5348(3)	0.82929(18)	0.0223(8)
O11	4*e*	-0.0667(6)	-0.5655(3)	0.85057(16)	0.0166(7)
O12	4*e*	0.2297(6)	-0.5090(3)	0.93667(16)	0.0176(7)
Ow13	4*e*	-0.3204(7)	-0.3611(3)	0.78262(17)	0.0197(8)
Ow14	4*e*	-0.7462(6)	-0.0536(3)	0.04872(16)	0.0162(7)
Ow15	4*e*	-0.6733(6)	-0.3827(3)	0.04510(16)	0.0154(7)
Ow16	4*e*	-0.2974(6)	-0.1165(3)	0.77258(16)	0.0184(8)
Ow17	4*e*	0.0498(7)	-0.2499(3)	0.73456(17)	0.0218(8)
H1	4*e*	-0.846(11)	-0.121(5)	0.034(3)	0.050*
H2	4*e*	-0.416(11)	-0.403(6)	0.808(3)	0.050*
H3	4*e*	-0.805(10)	-0.344(6)	0.020(3)	0.050*
H4	4*e*	0.070(12)	-0.311(6)	0.705(3)	0.050*
H5	4*e*	-0.327(12)	-0.106(7)	0.728(2)	0.050*
H6	4*e*	-0.393(12)	-0.371(7)	0.741(2)	0.050*
H7	4*e*	-0.401(11)	-0.064(6)	0.794(3)	0.050*
H8	4*e*	-0.733(12)	-0.386(7)	0.084(2)	0.050*
H9	4*e*	-0.727(12)	-0.064(7)	0.094(2)	0.050*
H10	4*e*	0.110(12)	-0.185(5)	0.711(3)	0.050*

*fixed during the refinement

https://doi.org/10.1180/mgm.2025.10165 Published online by Cambridge University Press

Table 5. Anisotropic displacement parameters (Å^2) of atoms in sarvodaite.

Atom	U^{11}	U^{22}	U^{33}	U^{23}	U^{13}	U^{12}
Al1	0.0138(7)	0.0075(7)	0.0114(7)	-0.0002(5)	0.0013(5)	-0.0005(5)
Al2	0.0085(9)	0.0085(9)	0.0097(9)	-0.0016(7)	-0.0006(7)	0.0014(7)
Al3	0.0103(9)	0.0063(9)	0.0116(9)	0.0013(7)	-0.0010(7)	-0.0019(7)
S1	0.0116(5)	0.0086(5)	0.0124(5)	0.0003(4)	0.0006(4)	0.0002(4)
S2	0.0120(5)	0.0063(5)	0.0131(5)	0.0004(4)	0.0011(4)	-0.0008(4)
S3	0.0129(5)	0.0087(5)	0.0132(5)	0.0002(4)	-0.0002(4)	0.0001(4)
O1	0.0188(18)	0.0105(17)	0.0246(19)	-0.0012(14)	-0.0019(14)	-0.0008(14)
O2	0.0177(18)	0.0197(19)	0.0168(17)	0.0022(14)	-0.0026(14)	0.0072(14)
O3	0.0139(16)	0.0088(17)	0.0238(18)	-0.0019(13)	0.0055(14)	-0.0011(12)
O4	0.0175(17)	0.0156(18)	0.0227(18)	0.0023(14)	0.0084(14)	-0.0011(14)
O5	0.0118(16)	0.0186(18)	0.0173(17)	0.0005(14)	0.0006(13)	0.0005(14)
O6	0.0219(18)	0.0140(17)	0.0173(17)	0.0026(13)	0.0068(14)	0.0048(14)
O7	0.0224(18)	0.0069(16)	0.0187(17)	-0.0004(13)	0.0037(14)	-0.0003(13)
O8	0.0162(18)	0.0152(18)	0.028(2)	-0.0004(15)	-0.0040(15)	-0.0007(14)
O9	0.0195(18)	0.0036(16)	0.032(2)	0.0029(14)	-0.0020(15)	0.0030(13)
O10	0.0252(19)	0.0133(18)	0.030(2)	-0.0037(15)	0.0122(16)	0.0011(14)
O11	0.0186(17)	0.0145(17)	0.0158(17)	0.0001(13)	-0.0023(13)	-0.0054(14)
O12	0.0169(17)	0.0181(18)	0.0171(17)	0.0007(14)	-0.0020(13)	-0.0041(14)
Ow13	0.0235(19)	0.0170(18)	0.0176(18)	0.0012(14)	-0.0018(14)	-0.0081(15)
Ow14	0.0163(18)	0.0177(18)	0.0154(17)	-0.0012(14)	0.0050(14)	-0.0054(14)
Ow15	0.0190(18)	0.0091(16)	0.0185(18)	0.0015(13)	0.0039(14)	0.0024(13)
Ow16	0.0248(19)	0.0175(19)	0.0127(17)	0.0036(14)	0.0017(14)	0.0097(14)
Ow17	0.033(2)	0.0124(18)	0.0214(19)	-0.0037(15)	0.0120(16)	-0.0014(16)

https://doi.org/10.1180/mgm.2025.10165 Published online by Cambridge University Press

Table 6. Selected interatomic distances (Å) in sarvodaite.

Al1-O9	1.865(3)	S1-O2	1.451(3)	Ow13-H2	0.91(4)
Al1-O6	1.866(4)	S1-O1	1.468(3)	Ow13-H6	0.91(4)
Al1-O1	1.890(4)	S1-O5	1.473(3)	Ow14-H1	0.94(4)
Al1-O16	1.890(4)	S1-O4	1.473(3)	Ow14-H9	0.94(4)
Al1-O17	1.890(4)			Ow15-H3	0.93(4)
Al1-O13	1.899(4)	S2-O8	1.441(3)	Ow15-H8	0.91(4)
		S2-O3	1.467(3)	Ow16-H5	0.93(4)
Al2-O14	1.870(3) ×2	S2-O7	1.473(3)	Ow16-H7	0.95(4)
Al2-O5	1.870(3) ×2	S2-O6	1.476(3)	Ow17-H4	0.92(4)
Al2-O3	1.893(3) ×2			Ow17-H10	0.94(4)
		S3-O10	1.456(4)		
Al3-O12	1.875(3) ×2	S3-O11	1.464(3)		
Al3-O15	1.895(3) ×2	S3-O12	1.478(3)		
Al3-O7	1.904(3) ×2	S3-O9	1.482(3)		

Table 7. Hydrogen bonds (*D* = donor, *A* = acceptor) in the structure of sarvodaite.

D–H···*A*	*d*(*D*–H)	*d*(H···*A*)	<*DHA*	*d*(*D*···*A*)
Ow14-H1···O8	0.94(4)	1.79(4)	168(4)	2.718(4)
Ow13-H2···O10	0.91(4)	1.98(4)	155(4)	2.838(4)
Ow15-H3···O8	0.93(4)	1.79(4)	163(4)	2.696(4)
Ow17-H4···O4	0.92(4)	1.73(4)	162(4)	2.622(4)
Ow16-H5···O11	0.93(4)	1.73(4)	167(4)	2.649(4)
Ow13-H6···O2	0.91(4)	1.77(4)	171(4)	2.679(4)
Ow16-H7···O4	0.95(4)	1.74(4)	174(4)	2.683(4)
Ow15-H8···O11	0.91(4)	1.92(4)	160(4)	2.787(4)
Ow14-H9···O2	0.94(4)	2.19(4)	130(4)	2.885(4)
Ow14-H9···O4	0.94(4)	2.1294)	135(4)	2.860(4)
Ow17-H10···O10	0.94(4)	1.84(4)	163(4)	2.759(4)

https://doi.org/10.1180/mgm.2025.10165 Published online by Cambridge University Press

Table 8. Bond-valence analysis* (in valence units = *v.u.*) for the crystal structure of sarvodaite.

	O1	O2	O3	O4	O5	O6	O7	O8	O9	O10	O11	O12		Ow13	Ow14	Ow15	Ow16	Ow17	∑
Al1	0.52					0.55			0.55					0.51			0.52	0.52	**3.17**
Al2			0.51×2→		0.55×2→										0.55×2→				**3.22**
Al3							0.50×2→					0.54×2→				0.51×2→			**3.10**
S1	1.52	1.58		1.50	1.50														**6.10**
S2			1.52			1.49	1.50	1.62											**6.13**
S3									1.46	1.56	1.53	1.48							**6.03**
								0.19					**H1**		0.81				**1.00**
										0.13			**H2**	0.87					**1.00**
								0.19					**H3**			0.81			**1.00**
				0.22									**H4**					0.78	**1.00**
											0.22		**H5**				0.78		**1.00**
		0.20											**H6**	0.80					**1.00**
				0.21									**H7**				0.79		**1.00**
											0.15		**H8**			0.85			**1.00**
		0.09		0.10									**H9**		0.81				**1.00**
										0.17			**H10**					0.83	**1.00**
∑	**2.04**	**1.87**	**2.03**	**2.03**	**2.05**	**2.04**	**2.00**	**2.00**	**2.01**	**1.86**	**1.90**	**2.02**		**2.18**	**2.17**	**2.17**	**2.09**	**2.13**	

**B.v.s. were calculated using the parameters from Gagné and Hawthorne, 2015.*

https://doi.org/10.1180/mgm.2025.10165 Published online by Cambridge University Press